

# Desorption Electrospray Ionization (DESI) Mass Spectrometric Imaging of Spatially Regulated *In Vivo* Metabolic Rates

Charlotte R. Lewis<sup>1</sup>, Richard H. Carson<sup>1</sup>, Mercede N. Erikson<sup>1</sup>, Anna P. Zagieboylo<sup>2</sup>, Bradley C. Naylor<sup>1</sup>, Kelvin W. Li<sup>3</sup>, John C. Price<sup>1</sup>, Paul B. Farnsworth<sup>1</sup>

<sup>1</sup>Department of Chemistry and Biochemistry, Brigham Young University, Provo, Utah 86402; <sup>2</sup>Current affiliation: Department of Molecular Biology, Massachusetts General Hospital, Boston, Massachusetts 02114; <sup>3</sup>Current affiliation: Department of Nutritional Sciences and Toxicology, University of California, Berkeley, California 94720

## I. ABSTRACT

Desorption electrospray ionization (DESI) is an ambient ionization technique used for mass spectrometric imaging of biological samples. When coupled with isotopic ratio measurements of deuterium-labeled tissues, DESI provides a means of measuring metabolic rates on a spatially resolved basis. *In vivo* metabolic rates are desired to better understand diseases such as Alzheimer's, Parkinson's, and Huntington's and to study the impact of space travel on muscle tissue growth and wasting. Although DESI has been used to image lipids and metabolites of a variety of tissues and other imaging techniques, such as NIMS, have been used to study kinetic turnover rates, DESI has not yet been used to study *in vivo* metabolic rates using deuterium labeled tissue. This paper describes how we optimized our DESI source for imaging of biological tissue, how we developed a MATLAB graphical user interface (GUI) to process and interpret the large mass spectral data files, and how we conducted our initial mouse brain study for proof-of-concept. Our initial mouse brain study involved labeling mice with deuterium enriched water, preparing tissue slices for DESI analysis, imaging the tissue slices using DESI coupled with a Bruker mass spectrometer, analyzing the mass spectral data using our custom-designed image\_inspector program, and creating incorporation curves to measure *in vivo* metabolic rates.

## II. INTRODUCTION

In 2004, R. Graham Cooks' research group introduced desorption electrospray ionization (DESI) (Figure 1) as a new ambient ionization method for mass spectrometry to simplify the sample introduction process.<sup>1</sup> Sample introduction systems for mass spectrometry have in the past been quite complex. For example, secondary ion mass spectrometry (SIMS)<sup>2</sup> requires that the sample be held under high vacuum. Matrix-assisted laser desorption/ionization (MALDI) requires careful sample pretreatment and is also usually conducted in an evacuated chamber.<sup>3</sup> The novelty of

DESI includes the ability to ionize compounds with little sample preparation and without a vacuum system. DESI involves spraying electrically charged solvent droplets onto a sample surface, accompanied by a high-velocity gas jet. The generally-accepted model for DESI analyte ionization involves analyte dissolving in a thin layer of the DESI solvent before being ejected in secondary droplets by impact from the primary spray.<sup>4</sup> The charged secondary droplets evolve into gas-phase ions similar to the theorized electrospray mechanism due to electrostatic and pneumatic forces.<sup>1</sup> The desorbed gas-phase ions are then sucked into a mass spectrometer for detection through a custom built electrically-charged metal inlet. With a soft-ionization mechanism, DESI can be used to see molecular ions of larger biological molecules as well as multiply-charged ions sampled directly from intact biological tissue.<sup>5</sup> The mass spectrum resembles that of electrospray ionization (ESI) because singly and multiply charged species are detected with little fragmentation. Cooks et al. demonstrated that DESI could be used to ionize both polar and nonpolar molecules including alkaloids, small drugs, peptides, and proteins that were present on varied surfaces that included metals, polymers, and minerals.<sup>1</sup>

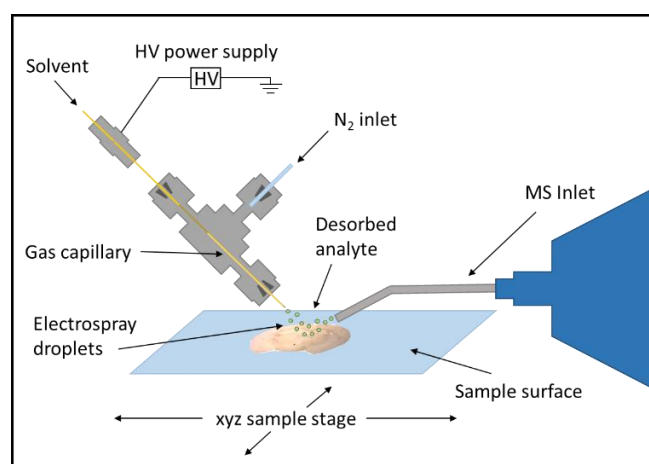


Figure 1: Schematic of Desorption Electrospray Ionization Mass Spectrometry (DESI-MS)

After the initial invention of DESI in 2004, the instrumentation, mechanisms and applications in forensics, chemistry, and biology were described by Cooks et al. in 2005.<sup>6</sup> The ionization mechanism is hypothesized to include aspects of both the heterogeneous charge-transfer mechanism as well as the droplet pick-up mechanism.<sup>6</sup> DESI can be used for qualitative as well as quantitative applications.

Many papers have been published in the last three years demonstrating the possibility of DESI imaging and DESI lipid profiling for human cancer and tumor applications. Research has been done to understand the repeatability and reproducibility of DESI imaging analysis of human cancer tissue.<sup>7</sup> Other research studies have focused on breast cancer margin analysis<sup>8</sup> and molecular typing of meningiomas for surgical decision-making.<sup>9</sup>

Although many studies had been done to understand deuterium enrichment in the lipids of rats,<sup>10,11</sup> the first study to determine the maximum incorporation number (N) of deuteriums in the synthesis of stearate, palmitate, and cholesterol was Lee et al.<sup>12</sup> This study showed that mass isotopomer analysis after feeding rats deuterium-enriched water could be used to understand the replacement rate of lipids found in various organs in the body to help elucidate the synthetic pathways of specific lipids of interest.

Although DESI has been used to image lipids and metabolites of a variety of tissues<sup>13</sup> and other imaging techniques such as NIMS have been used to study kinetic turnover rates,<sup>10</sup> DESI has not yet been used to study *in vivo* metabolic rates using deuterium labeled tissue.

### III. METHODS/PROCEDURE

The desorption electrospray ionization mass spectrometry (DESI-MS) source, used to acquire mass spectrometric images of mouse brains contained within this thesis, consisted of a DESI emitter, a solvent syringe and pump system, a high voltage power supply, a cylinder of compressed nitrogen, a motorized, programmable translational stage, a glass slide mount, a microscope eyepiece, a light source, and a mass spectrometer with a customized sniffer inlet. The DESI emitter was custom built from a 1/16 inch Swagelok T. The emitter tip consisted of a 4-cm-long spray capillary emitter purchased from Prosofia Scientific (0.05 in ID and 0.15 in OD, Indianapolis, IN, U.S.A.) that was superglued (Loctite 404) into PEEK

tubing (us.vwr.com). The PEEK tubing was used to connect the Prosofia capillary emitter to the high voltage connector and then to the solvent syringe (Hamilton 500  $\mu$ L, Model 1750 CX SYR, 1/4-28 Threads). The syringe was pumped with a Harvard pump (Harvard Apparatus PHD 2000, Holliston, MA, U.S.A.) at a solvent flow rate of 1-3  $\mu$ L/min. Plastic tubing delivered the compressed nitrogen (Airgas, Salt Lake City, UT, U.S.A.) to the Swagelok T at 160 psi. The gas exited the Swagelok T through an approximately 2-cm-long fused silica capillary (182  $\mu$ m ID and 354  $\mu$ m OD, Molex, Polymicro Technologies, Phoenix, AZ, U.S.A.) that coaxially surrounded the Prosofia spray capillary emitter. The Prosofia capillary emitter extended out past the gas capillary approximately 0.5 mm. The emitter tip to sample surface distance was approximately 1 mm, but was optimized for each tissue scan. The emitter tip to mass spectrometer inlet distance was approximately 4-5 mm. The DESI emitter angle was 55 degrees relative to the tissue surface.

High voltage (Stanford Research Systems, Inc. Model PS350, Sunnyvale, CA, U.S.A.) of -5kV was applied to the high voltage no-dead-volume connector to electrically charge the methanol solvent. A microscope eyepiece (Nikon, Melville, NY, U.S.A.) was used to view the DESI emitter tip and the DESI solvent spray spot on the tissue. Our light source (Cole-Palmer Illuminator, Model 41722, Vernon Hills, IL, U.S.A.) was simply used to illuminate the tissue samples on the glass slides to better see contrast with the microscope eyepiece. A custom machined glass slide mount was used to hold the tissue samples on the motorized, programmable translational stage (Prior Scientific, Rockland, MA, U.S.A.), which communicated with the MicroTOF II mass spectrometer (Bruker Daltonics, Billerica, MA, U.S.A.) to raster the tissue samples and obtain mass spectral data, one pixel (75  $\mu$ m  $\times$  150  $\mu$ m) at a time. Ions entered the mass spectrometer through a custom-adapted stainless steel sniffer that had a collection angle of 18 degrees (the angle  $\beta$  in Figure 3). The mass spectrometer was run in negative ion mode with an inlet voltage of 500 V, which was applied to the glass transfer capillary. The mass range was approximately 200-900 m/z. All these instrumental parameters are summarized in Table 1 and Table 2. Figure 2 contains two photographs with most of the DESI-MS elements labeled. Geometry parameters for our DESI source are diagrammed in Figure 3 and included in Table 2.

Table 1: DESI Imaging Parameters

Parameter	Setting
N <sub>2</sub> Gas Pressure	160 psi
Solvent Type	100% methanol
Solvent Flow Rate	1-3 $\mu\text{L}/\text{min}$
Applied Solvent Voltage	-5 kV
Mass Range	200 to 900 m/z
Ion Polarity	Negative
MS Inlet Voltage	500 V
Mass Spectra Rolling Average	2
Mass Spectra Rate	1 Hz
Pixel Size	75 $\mu\text{m}$ $\times$ 150 $\mu\text{m}$

Table 2: DESI Geometry Parameters

Parameter	Description	Value
$\alpha$	DESI probe angle	55°
$\beta$	sniffer inlet angle	18°
$d_1$	capillary tip extension	0.5 mm
$d_2$	capillary tip to surface distance	1-2 mm
$d_3$	capillary tip to sniffer inlet distance	4-5 mm
$d_4$	sniffer inlet to surface distance	< 1 mm

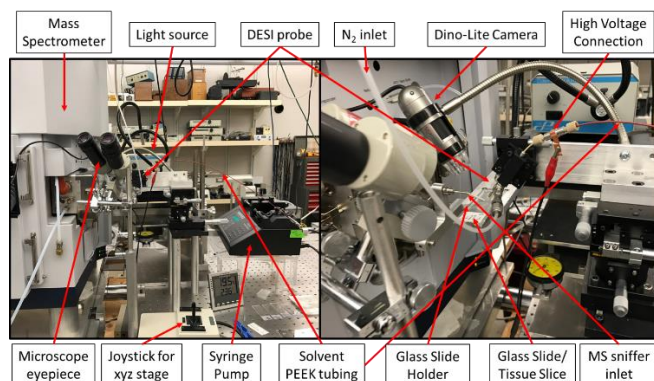


Figure 2: Photographs of the DESI-MS setup with Labels

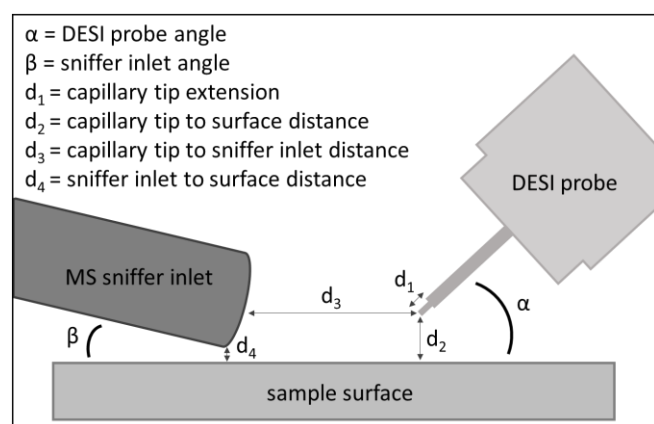


Figure 3: Diagram of DESI Geometry Parameters

Collaborating with Dr. John C. Price's research group, we used DESI mass spectrometric imaging to measure spatially regulated *in vivo*

metabolic rates in mice. I was responsible for the DESI imaging and isotope ratio processing. The Price lab was responsible for properly labeling the mice with deuterium by altering their water intake, reproducibly slicing brain and other tissue using a cryostat, thaw mounting the tissue slices to glass slides, and helping determine the incorporation rates of individual lipids after DESI imaging. The work flow of the research is outlined in Figure 4 with the Price lab responsible for step one and step six. Steps two through five were primarily my responsibility.

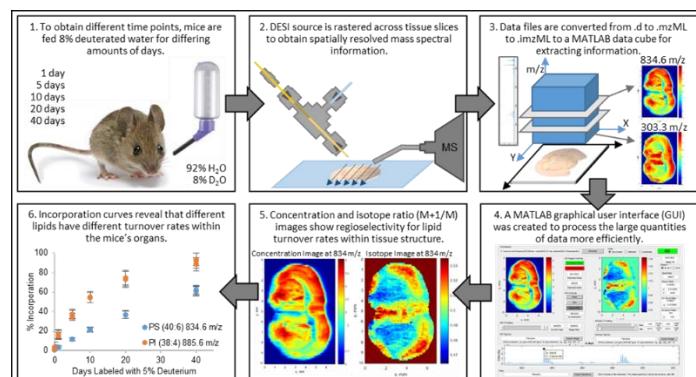


Figure 4: DESI Research Workflow

A Bruker MicrOTOF II mass spectrometer coupled with our laboratory-constructed DESI source, was used to acquire DESI images. Our motorized, programmable translational stage communicated with the mass spectrometer to raster the tissue samples and obtain mass spectral data one pixel at a time as seen in Figure 5. A custom-machined glass slide mount was used to hold the tissue samples in place on the stage.

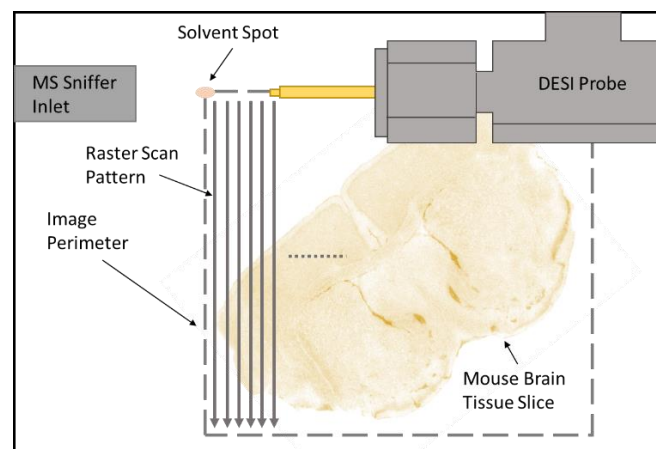


Figure 5: Raster Pattern for DESI Imaging

#### IV. SOFTWARE DEVELOPMENT

During each DESI tissue scan, the Bruker MicrOTOF II mass spectrometer saved each row of

tissue information to an individual file with a .d file extension. Free downloadable processing programs (msconvert<sup>14</sup> and imzML Converter<sup>15,16</sup>) were used to convert the .d original acquisition files to .mzML files and ultimately to a single .imzML file. Then this condensed .imzML file was converted into a MATLAB datacube using an adapted version of Georgia Tech’s imzml\_to\_cube<sup>17</sup> MATLAB program. Paul Farnsworth created a program called image\_inspector to allow users easy access to the mass spectral and image data in the data cube. His program incorporated some elements of another Georgia Tech MATLAB program.<sup>17</sup> Finally, I added the isotope ratio capability, statistical analysis, region of interest saver, and other features to Dr. Farnsworth’s program to create the current version of image\_inspector.

The final datacube has four dimensions of data: x coordinate, y coordinate, m/z, and signal intensity. Mass spectral information was collected for each pixel for the entire brain tissue slice. For each x,y coordinate position, there is an entire mass spectrum which has signal intensity for each data point ranging from 200 to 900 m/z. Figure 6 demonstrates how the datacube can be imagined as a stack of ion intensity images for each m/z value.

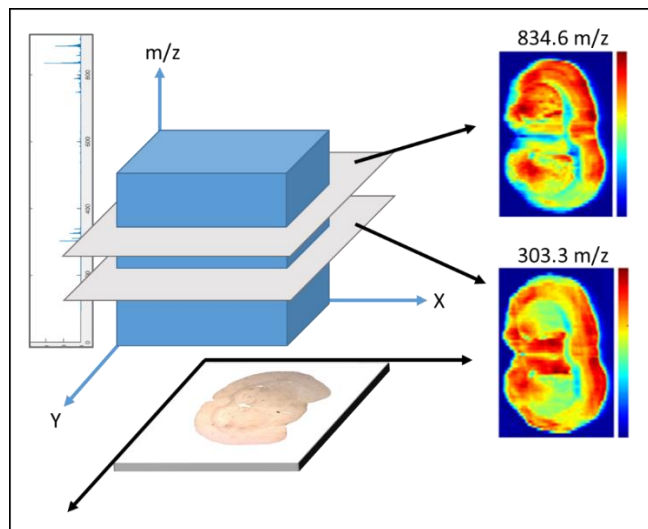


Figure 6: MATLAB Datacube

An averaged mass spectrum for the entire DESI scan appears at the bottom of the GUI as seen in Figure 7. When a region of interest (ROI) or a single pixel is selected, a new mass spectrum appears. In the case of a single pixel, the mass spectrum is for that pixel. For an ROI selection, the spectrum is the average of the spectra from the pixels within the ROI boundaries. Peaks in the averaged mass spectrum can

be selected to show a concentration image of the entire brain scan at the selected mass.

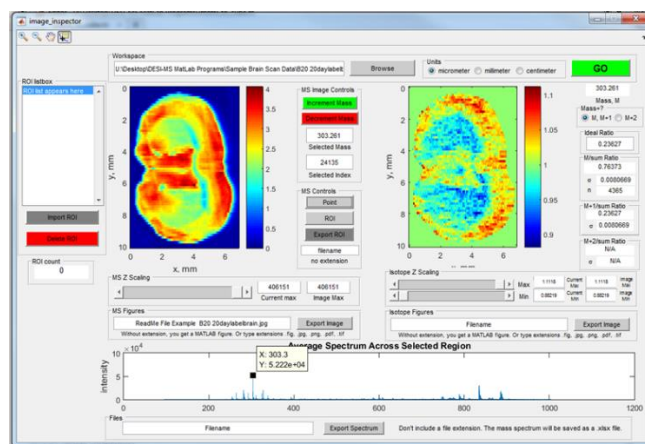


Figure 7: image\_inspector Graphical User Interface (GUI)

When a peak is selected from the averaged mass spectrum and the “Point” button is clicked, a concentration image is generated on the left-hand side of the GUI. This concentration image is created by summing the area beneath the selected peak for each individual pixel. The area is calculated by summing the intensity of 12 points above and below the center of the selected point. The number of points to be included in the area was determined by looking at the 303.3 m/z peak as well as the 834.6 m/z peak and ensuring the entire peak area was included without including neighboring peaks. The colormap is determined by setting the maximum pixel intensity to red and the lowest pixel intensity to dark blue. “Jet” was the chosen among possible MATLAB color schemes for the colormap. The color scaling of the concentration image is manipulated by using the “MS Z scaling” panel which changes the maximum scale value corresponding to red.

Creating the isotope ratio image on the right-hand side of the GUI was more complex than displaying a concentration map. The idea of the isotope ratio image came from wanting to see if deuterium was regioselectively incorporated by different lipids and fatty acids and to see if the rates of incorporation could be measured. Figure 8 shows the mass isotopomer of phosphatidylserine (40:6) (834.6 m/z). As deuterium was incorporated into the body, the mass isotopomer pattern of the lipid changed due to the heavy nature of deuterium compared to hydrogen. As illustrated in Figure 8, the sample from a mouse that had been on a deuterium enriched diet for forty day has an

isotopomer distribution shifted to higher masses compared to the unlabeled sample. The isotope ratio image was designed to calculate the ratio of the M peak to the M+1 peak and show the isotope ratios visually for each DESI scan of brain tissue.

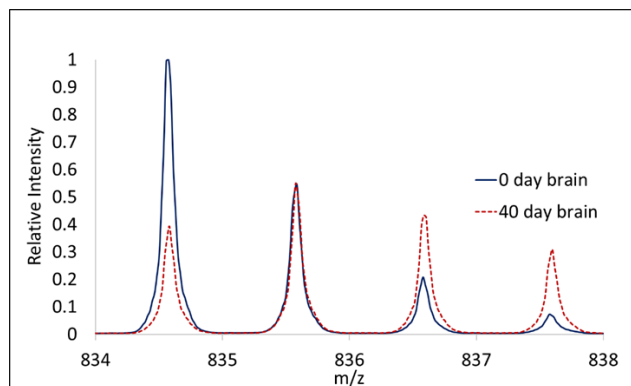


Figure 8: Mass Isotopomer of Phosphatidylserine at 834.6 m/z

The region of interest (ROI) button was designed initially to generate an averaged mass spectrum from only those pixels located within the ROI boundaries. Now that the isotope ratio image has been incorporated, the ROI button calculates an averaged isotope ratio and the standard deviation of that ratio for all the pixels within the ROI. The “ROI listbox” located on the far-left side of the GUI as seen in Figure 7 saves any regions of interest to be recalled at a later date. When a ROI is selected and uploaded, the isotope ratio is recalculated and the averaged mass spectrum is graphed.

## V. RESULTS/DISCUSSION

After the DESI source was used to image the mouse brains, MATLAB was used to process the large mass spectral data files and create concentration and isotope ratio images with color maps for visual appeal and clarity. Four lipids were selected for detailed study because they had the highest intensities in the mass spectrum, unique regio-spatial concentration patterns, tentative assignments from another published research study,<sup>8</sup> and mostly clean M+1 peaks for monitoring isotope ratio changes. An arachidonic acid isomer (AA), docosahexaenoic acid (DHA), phosphatidylserine 40:6 (PS), and phosphatidylinositol 38:4 (PI) were the four lipids highlighted in this research study as seen in Figure 9, Figure 10, Figure 11, and Figure 12, respectively. The first two columns in these four figures contain isotope ratio images with

burgundy backgrounds. The last column contains concentration images with a blue background.

Signal intensity in the DESI images for a chosen m/z value is directly related to the concentration of that compound. However, signal intensity is also affected by the tissue type, optimization of DESI parameters, tissue surface roughness, and changes in the surrounding atmosphere during a DESI scan. Although many variables affected the consistency of the signal intensity, with variations particularly noticeable in the concentration images, the spatial distribution of the lipids was consistent with classical brain structures for each of the four targeted lipids. For instance, the signal intensity of PS (Figure 11, right column) in the DESI images for all time points of the experiment showed that the relative concentration of PS was higher in the cerebral cortex and caudoputamen and lower in the corpus callosum.

When comparing the changes in the signal intensities in the concentration images with the changes in the isotope ratios for the four lipids, we noticed they are not necessarily linked, particularly for AA, PS, and PI (Figure 9, Figure 11, Figure 12). If we look at the isotope ratio images that have been scaled linearly for the entire 40-day-long experiment (global scaling), we see a change in color for the entire brain, suggesting that new lipid is being synthesized throughout the entire organ. Looking at the isotope ratio images that are scaled to emphasize variations within each image (independent scaling), we notice small but measurably faster turnover rates in different parts of the brain for individual lipids. The symmetry of each isotope ratio image resembles the structure of a typical mouse brain, which reduces the possibility that transient fluctuations are responsible for the changes. The isotope ratio images are much more robust than the concentration images because ionization efficiency does not affect the isotopomer distribution ratios. Heavy and light versions of each lipid are chemically identical to one another and therefore respond the same during DESI imaging.

AA (Figure 9) was observed to have relatively high concentrations everywhere in the brain tissue except for parts of the caudoputamen region and the corpus callosum. Lipid turnover rates were observed to be slower in the caudoputamen and corpus callosum regions as well. This correlation suggests that AA is synthesized and degraded locally.

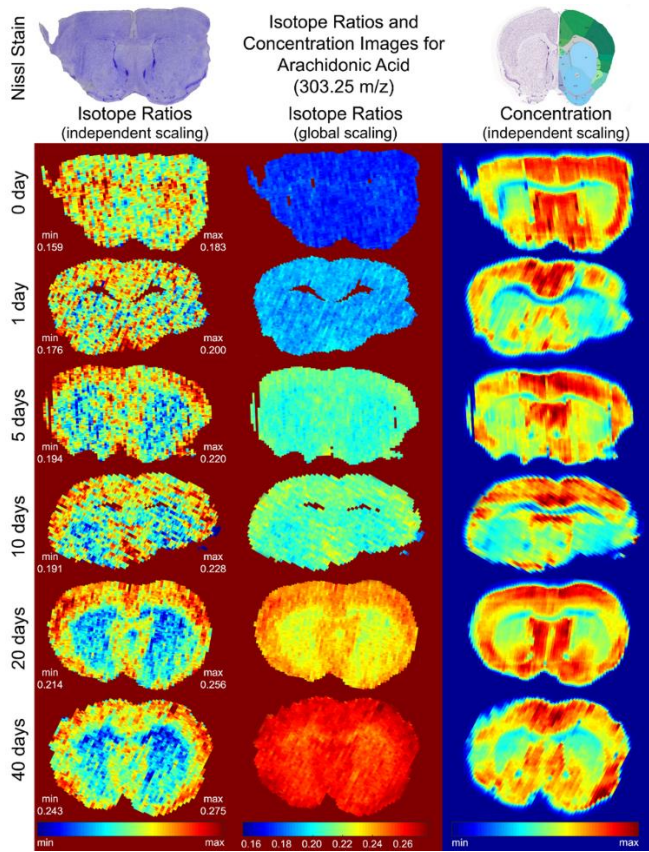


Figure 9: Concentration and Isotope Ratio Images for 303.25

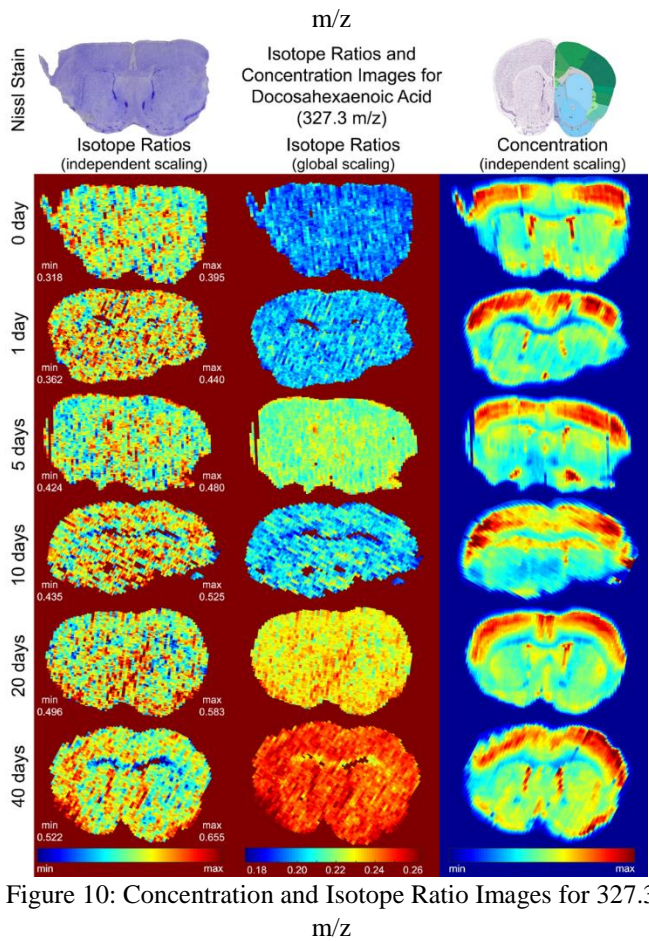


Figure 10: Concentration and Isotope Ratio Images for 327.3

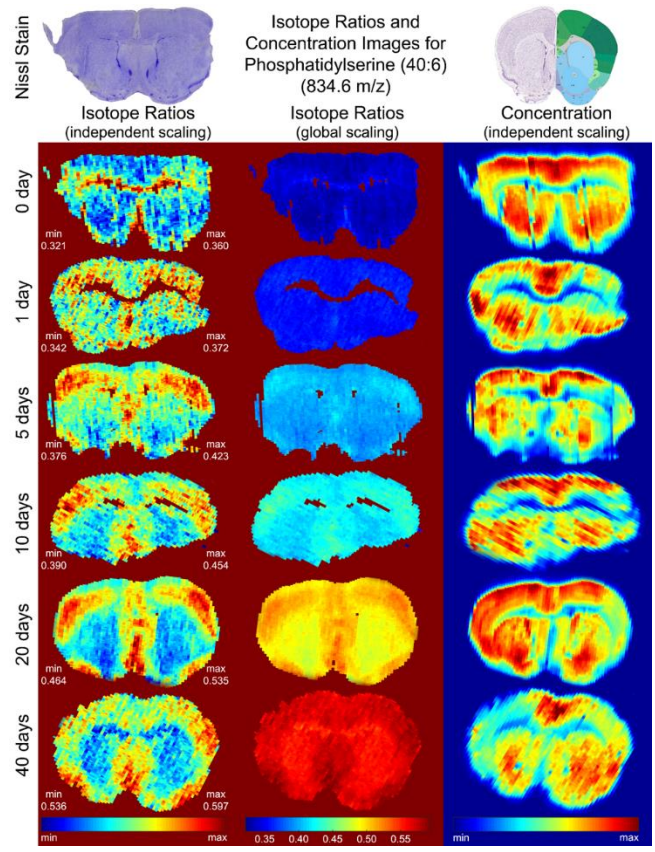


Figure 11: Concentration and Isotope Ratio Images for 834.6

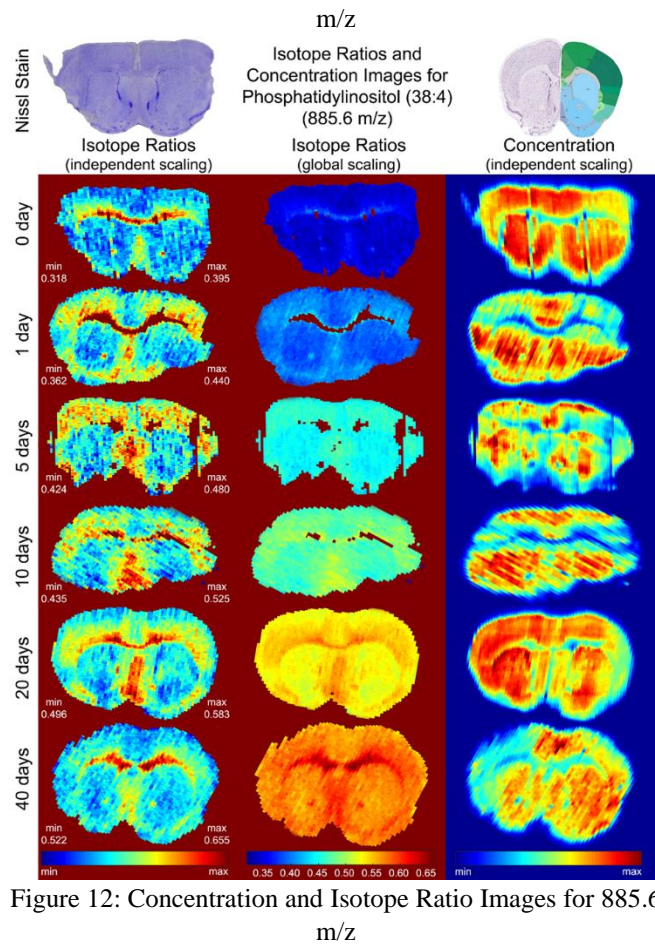


Figure 12: Concentration and Isotope Ratio Images for 885.6

DHA (Figure 10) was found mostly in the cerebral cortex. Unlike the other three lipids studied here, DHA had a very small change in the isotope ratio suggesting that lipid turnover is minimal throughout the entire brain. DHA is considered conditionally essential in the diet and so these results were not surprising. Noisy isotope ratio images, particularly noticeable in the global scaling column, were partially caused by a background peak interfering with the M+1 peak. When the background peak varied in intensity from scan to scan, the linearity of the global scaling for the isotope ratio images was noticeably affected.

Looking at the independent scaling of the isotope ratio images for PS (Figure 11), there was a small but measurably faster turnover rate in the septal nucleus and a subsection of the cerebral cortex. Slightly slower turnover was observed in the caudoputamen region and corpus callosum. The concentration images revealed relatively high concentrations of PS throughout the entire brain except for the corpus callosum.

PI (Figure 12) was observed to have similar concentration images to PS. Relatively high PI concentrations were found throughout the entire brain except for the corpus callosum. However, the isotope ratio images for PI varied dramatically from the isotope ratio images for PS. The fast turnover occurred in the corpus callosum where the concentration was relatively low. Therefore, the body must either synthesize and immediately degrade this lipid locally in the corpus callosum or the body synthesizes and distributes this lipid to the surrounding areas from the corpus callosum.

Figure 13, Figure 14, and Table 3 were created by Richard Carson and Dr. John C. Price. These figures and this table are used with permission to explain how DESI imaging was used to measure *in vivo* metabolic rates.

Figure 13 shows how the experimental and simulated mass isotopomer distribution changed over time as more deuterium was incorporated into a mouse's lipids. The initial isotopomer distribution pattern at time point zero days came from the natural isotope abundances of carbon, nitrogen, oxygen, and hydrogen. Over time, the main mass peak (M0) intensity decreased and the M+1 (M1) and M+2 (M2) peak intensities increased as more deuterium was incorporated from the deuterium enriched drinking water. We calculated the number of covalent deuteriums sites (n) for each lipid (Table 3) after we

measured the D<sub>2</sub>O enrichment in the mice and optimized the isotopomer simulation to match the experimental data. AA, PS, and PI each had a single best n value that minimized the deviation between the experimental and theoretical isotopomer distributions, as previously described.<sup>11,18</sup> We could not determine a unique n value for DHA because this lipid had a small overall change in the isotopomer distribution and had interferences from nearby molecules.

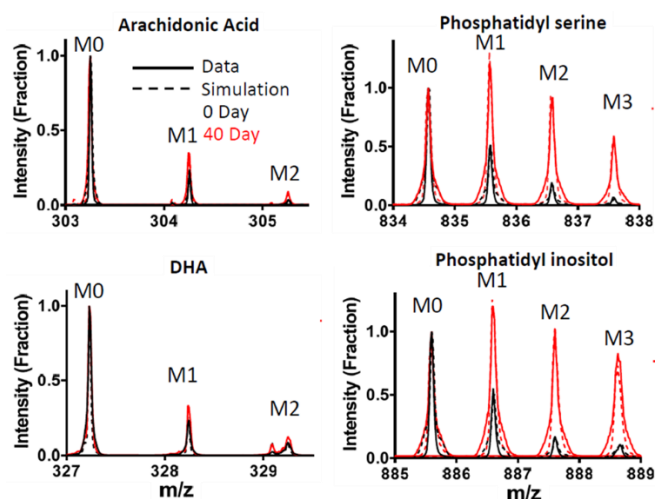


Figure 13: Comparison of Experimental and Optimized Simulations of Lipid Isotopomers

High-resolution mass spectra were used to measure independent turnover rates (k) for multiple lipids simultaneously. These calculations were previously described for peptides by Price<sup>18,19</sup> and others,<sup>20,21</sup> but this was the first time lipid turnover rates were measured using DESI-MS. Turnover rates (k) for the cerebral cortex (CO) and caudoputamen (CA) regions of the brain were calculated by averaging the mass spectra in those regions using our image\_inspector program and using the scipy package in python for the recursive, non-linear regression fit. Differences in the calculated k values for the CA and CO regions were statistically significant for AA, DHA, and PS as seen by the asterisks in Table 3.

Figure 14 shows the kinetic curves for each of the four major singly-charged ions observed in our DESI mass spectra. The kinetic curves show that lipids vary in their turnover rates as well as their percentages of biosynthesized lipid compared to dietary lipid. As lipids are biosynthesized within the body, protons and deuteriums are incorporated from the water available within the body. The number of deuteriums incorporated depends on the deuterium enrichment of the body water at that time, which was measured from

the urine and plasma of each mouse. Table 3 summarizes the common lipid name, observed ionic mass, elemental composition, number of deuterium sites, calculated turnover rates for the CA and CO regions, and the percentage of biosynthesized compared to dietary lipid for the four lipids in this study.

More details on calculating the  $n$  values and  $k$  values for each of these four lipids can be obtained from Richard Carson and Dr. John C. Price. A brief summary has been provided here in this paper to help describe the collaborative efforts of using DESI-MS imaging for measuring spatially regulated *in vivo* metabolic rates.

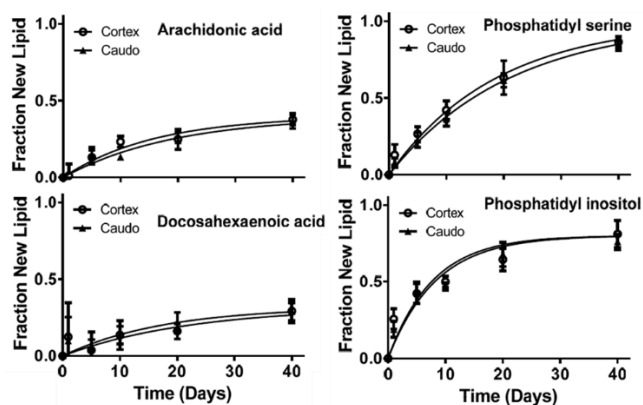


Figure 14: Kinetic Curves for the Four Lipids: AA, DHA, PS, and PI

Table 3: Common Name, Observed Ionic Mass, Elemental Composition, Number of Deuteriums, Turnover Rates, and Percentage of Biosynthesized Lipid for the Four Major Singly Charged Ions Observed in our DESI-MS Spectra

Lipid	m/z	Formula	n	k in CA	k in CO	%
Arachidonic Acid*	303.25	C <sub>20</sub> H <sub>32</sub> O <sub>2</sub>	6	0.051±0.005	0.063±0.007	40
Docosahexaenoic Acid*	327.25	C <sub>22</sub> H <sub>32</sub> O <sub>2</sub>	~8	0.057±0.019	0.045±0.010	32
Phosphatidylserine*	834.6	C <sub>46</sub> H <sub>77</sub> NO <sub>10</sub> P	21	0.053±0.003	0.047±0.001	100
Phosphatidylinositol	885.6	C <sub>47</sub> H <sub>82</sub> O <sub>13</sub> P	27	0.121±0.012	0.129±0.016	76

## VI. CONCLUSIONS

This paper highlighted our recent advancements for DESI mass spectrometric imaging including optimization of DESI parameters, spatial detection of lipids and fatty acids in mouse brains, and *in vivo* metabolic rate calculations for future disease and muscle wasting analysis. We developed a MATLAB program, `image_inspector`, to help us view and understand data acquired from DESI imaging. We measured metabolic rates of lipids and fatty acids within the brain by observing changes in isotopomer patterns. We confirmed lipid assignments using

MS/MS fragmentation patterns. We created incorporation curves from data measured in the isotope ratio images and determined the number of exchange sites for multiple lipids. We hope our progress in DESI mass spectrometric imaging can contribute in the future to the application of DESI imaging in the various fields of neuroscience, pharmacology, clinical pathology, oncology, and space travel.

## VII. ACKNOWLEDGEMENTS

I would like to thank the Department of Chemistry and Biochemistry at Brigham Young University and the Utah NASA Space Grant Consortium (UNSGC) for funding.

## VIII. REFERENCES

1. Takats, Z.; Wiseman, J. M.; Gologan, B.; Cooks, R. G. Mass spectrometry sampling under ambient conditions with desorption electrospray ionization. *Science* **2004**, *306*, 471-473.
2. Brunelle, A.; Touboul, D.; Laprevote, O. Biological tissue imaging with time-of-flight secondary ion mass spectrometry and cluster ion sources. *J. Mass Spectrom.* **2005**, *40*, 985-999.
3. Caprioli, R. M.; Farmer, T. B.; Gile, J. Molecular imaging of biological samples: Localization of peptides and proteins using MALDI-TOF MS. *Anal. Chem.* **1997**, *69*, 4751-4760.
4. Costa, A. B.; Cooks, R. G. Simulation of atmospheric transport and droplet-thin film collisions in desorption electrospray ionization. *Chemical Communications* **2007**, 3915-3917.
5. Wiseman, J. M.; Puolitaival, S. M.; Takats, Z.; Cooks, R. G.; Caprioli, R. M. Mass spectrometric profiling of intact biological tissue by using desorption electrospray ionization. *Angewandte Chemie-International Edition* **2005**, *44*, 7094-7097.
6. Takats, Z.; Wiseman, J. M.; Cooks, R. G. Ambient mass spectrometry using desorption electrospray ionization (DESI): instrumentation, mechanisms and applications in forensics, chemistry, and biology. *J. Mass Spectrom.* **2005**, *40*, 1261-1275.
7. Abbassi-Ghadi, N.; Jones, E. A.; Gomez-Romero, M.; Golf, O.; Kumar, S.; Huang, J. Z.; Kudo, H.; Goldin, R. D.; Hanna, G. B.; Takats, Z. A Comparison of DESI-MS and LC-MS for the Lipidomic Profiling of Human Cancer Tissue. *J. Am. Soc. Mass Spectrom.* **2016**, *27*, 255-264.
8. Calligaris, D.; Caragacianu, D.; Liu, X. H.; Norton, I.; Thompson, C. J.; Richardson, A. L.; Golshan, M.; Easterling, M. L.; Santagata, S.; Dillon, D. A.; Jolesz, F. A.; Agar, N. Y. R. Application of

- desorption electrospray ionization mass spectrometry imaging in breast cancer margin analysis. *Proc. Natl. Acad. Sci. U. S. A.* **2014**, *111*, 15184-15189.
9. Calligaris, D.; Feldman, D. R.; Norton, I.; Brastianos, P. K.; Dunn, I. F.; Santagata, S.; Agar, N. Y. R. Molecular typing of meningiomas by desorption electrospray ionization mass spectrometry imaging for surgical decision-making. *International Journal of Mass Spectrometry* **2015**, *377*, 690-698.
10. Louie, K. B.; Bowen, B. P.; McAlhany, S.; Huang, Y. R.; Price, J. C.; Mao, J. H.; Hellerstein, M.; Northen, T. R. Mass spectrometry imaging for in situ kinetic histochemistry. *Sci. Rep.* **2013**, *3*.
11. Price, J. C.; Khambatta, C. F.; Li, K. W.; Bruss, M. D.; Shankaran, M.; Dalidd, M.; Floreani, N. A.; Roberts, L. S.; Turner, S. M.; Holmes, W. E.; Hellerstein, M. K. The Effect of Long Term Calorie Restriction on in Vivo Hepatic Proteostasis: A Novel Combination of Dynamic and Quantitative Proteomics. *Mol. Cell. Proteomics* **2012**, *11*, 1801-1814.
12. Lee, W. N. P.; Bassilian, S.; Ajje, H. O.; Schoeller, D. A.; Edmond, J.; Bergner, E. A.; Byerley, L. O. In-Vivo Measurement of Fatty-acids and Cholesterol-synthesis Using D2O and Mass Isotopomer Analysis. *Am. J. Physiol.* **1994**, *266*, E699-E708.
13. Wiseman, J. M.; Ifa, D. R.; Song, Q. Y.; Cooks, R. G. Tissue imaging at atmospheric pressure using desorption electrospray ionization (DESI) mass spectrometry. *Angewandte Chemie-International Edition* **2006**, *45*, 7188-7192.
14. Kessner, D.; Chambers, M.; Burke, R.; Agus, D.; Mallick, P. ProteoWizard: open source software for rapid proteomics tools development. *Bioinformatics* **2008**, *24*, 2534-2536.
15. Race, A. M.; Styles, I. B.; Bunch, J. Inclusive sharing of mass spectrometry imaging data requires a converter for all. *J. Proteomics* **2012**, *75*, 5111-5112.
16. Schramm, T.; Hester, A.; Klinkert, I.; Both, J.-P.; Heeren, R. M. A.; Brunelle, A.; Laprévotte, O.; Desbenoit, N.; Robbe, M.-F.; Stoeckli, M.; Spengler, B.; Römpf, A. imzML — A common data format for the flexible exchange and processing of mass spectrometry imaging data. *J. Proteomics* **2012**, *75*, 5106-5110.
17. Parry, R. M.; Galhena, A. S.; Gamage, C. M.; Bennett, R. V.; Wang, M. D.; Fernandez, F. M. OmniSpect: An Open MATLAB-Based Tool for Visualization and Analysis of Matrix-Assisted Laser Desorption/Ionization and Desorption Electrospray Ionization Mass Spectrometry Images. *J. Am. Soc. Mass Spectrom.* **2013**, *24*, 646-649.
18. Price, J. C.; Holmes, W. E.; Li, K. W.; Floreani, N. A.; Neese, R. A.; Turner, S. M.; Hellerstein, M. K. Measurement of human plasma proteome dynamics with 2H2O and liquid chromatography tandem mass spectrometry. *Anal. Biochem.* **2012**, *420*, 73-83.
19. Price, J. C.; Guan, S. H.; Burlingame, A.; Prusiner, S. B.; Ghaemmaghami, S. Analysis of proteome dynamics in the mouse brain (vol 107, pg 14508, 2010). *Proc. Natl. Acad. Sci. U. S. A.* **2014**, *111*, 3645-3645.
20. Kasumov, T.; Ilchenko, S.; Li, L.; Rachdaoui, N.; Sadygov, R. G.; Willard, B.; McCullough, A. J.; Previs, S. Measuring protein synthesis using metabolic (<sup>2</sup>H) labeling, high-resolution mass spectrometry, and an algorithm. *Anal. Biochem.* **2011**, *412*, 47-55.
21. Lam, M. P. Y.; Wang, D.; Lau, E.; Liem, D. A.; Kim, A. K.; Ng, D. C. M.; Liang, X.; Bleakley, B. J.; Liu, C.; Tabaraki, J. D.; Cadeiras, M.; Wang, Y.; Deng, M. C.; Ping, P. Protein kinetic signatures of the remodeling heart following isoproterenol stimulation. *The Journal of Clinical Investigation* **2014**, *124*, 1734-1744.